Impact of Aerodynamics and Structures Technology on Heavy Lift Tiltrotors

C. W. Acree, Jr.
Aerospace Engineer
NASA Ames Research Center
Moffett Field, CA
cecil.w.acree@nasa.gov

Abstract

Rotor performance and aeroelastic stability are presented for a 124,000-lb Large Civil Tilt Rotor (LCTR) design. It was designed to carry 120 passengers for 1200 nm, with performance of 350 knots at 30,000 ft altitude. Design features include a low-mounted wing and hingeless rotors, with a very low cruise tip speed of 350 ft/sec. The rotor and wing design processes are described, including rotor optimization methods and wing/rotor aeroelastic stability analyses. New rotor airfoils were designed specifically for the LCTR; the resulting performance improvements are compared to current technology airfoils. Twist, taper and precone optimization are presented, along with the effects of blade flexibility on performance. A new wing airfoil was designed and a composite structure was developed to meet the wing load requirements for certification. Predictions of aeroelastic stability are presented for the optimized rotor and wing, along with summaries of the effects of rotor design parameters on stability.

Notation

A	rotor disk area
c.g.	center of gravity
c_l	section lift coefficient
c_m	section pitching moment coefficient
C_T	rotor thrust coefficient, $T/(\rho A V^2_{tip})$
D	drag
F_c	fuel consumed
FM	figure of merit
M	Mach number
q	dynamic pressure
R	rotor radius
Re	Reynolds number
t/c	thickness to chord ratio
T	rotor thrust
V_{tip}	rotor tip speed
η	propulsive efficiency
ρ	air density
σ	rotor solidity (ratio blade area to disk area)
ISA	international standard atmosphere
LCTR	Large Civil Tilt Rotor
OEI	one engine inoperative
SFC	specific fuel consumption
SNI	simultaneous non-interfering
SOA	state of the art
VTOL	vertical takeoff and landing

Introduction

The NASA Heavy Lift Rotorcraft Systems Investigation studied several candidate configurations of very large rotorcraft designed for the civil mission (Refs. 1, 2). With gross weights in excess of 100,000 lb and speeds of 350 knots or greater, such aircraft will face severe design challenges to meet acceptable performance and safety requirements. The Large Civil Tilt Rotor (LCTR) is the most promising design resulting from the investigation. This paper addresses the optimization and analysis of the LCTR, covering rotor and wing design and presenting results for performance and stability.

Whirl flutter is a major technology driver for tiltrotors. Therefore, careful attention must be given to the wing design process to ensure a stable and efficient solution. The task is compounded by the impact of rotor design on whirl flutter. The rotor designer faces conflicting requirements: articulated and soft-in-plane rotors have low loads but poor stability, whereas hingeless (stiff-in-plane) rotors have high loads and good stability. Gimballed rotors, as used on the XV-15, V-22 and BA-609, do not scale well to four or more blades because of kinematic constraints. A low wing layout may dictate hingeless rotors for adequate pitch control in hover, at the expense of high loads. Therefore, the wing and rotor cannot be designed independently of each other.

Three major sets of design requirements drive the LCTR analyses addressed here. Performance goals for hover and cruise determine the rotor size and disk loading and set the wing area and maximum thickness. Loads determine rotor and wing structural designs, which must be analyzed for aeroelastic stability. Performance, loads and stability requirements for both the rotor and wing influence each other during the design process, requiring an iterative optimization process (Refs. 1, 2). In this paper, the design approach and its implications for tiltrotor technology are divided into three general areas: rotor design for performance, wing design for loads, and coupled wing/rotor aeroelastic stability (whirl flutter).

This paper begins with a summary of aircraft design requirements for the LCTR. The iterative rotor design process is described, beginning with a summary of sizing results and airfoil design. There follows a discussion of twist optimization and the effects of structural stiffness on performance, then the analysis is extended to include interactions between taper and precone during performance optimization. A discussion of the wing design follows, with attention given to loads requirements and whirl-mode stability. The paper concludes with suggestions for research for very large tiltrotors.

LCTR Conceptual Design

The Large Civil Tiltrotor (LCTR) is illustrated in Fig. 1. Key design values are summarized in Table 1. The objectives of the LCTR design are to be competitive with regional jets and compatible with future, crowded airspace. The baseline civil mission is defined by NASA technology goals (Ref. 1) and is summarized in Table 2. The LCTR is designed for 350 knots at 30,000 ft altitude, with low disk loading in hover. It has a low cruise tip speed of 350 ft/sec for high efficiency and a hover tip speed of 650 ft/sec for low noise. Further design details are given in Refs. 1 and 2.

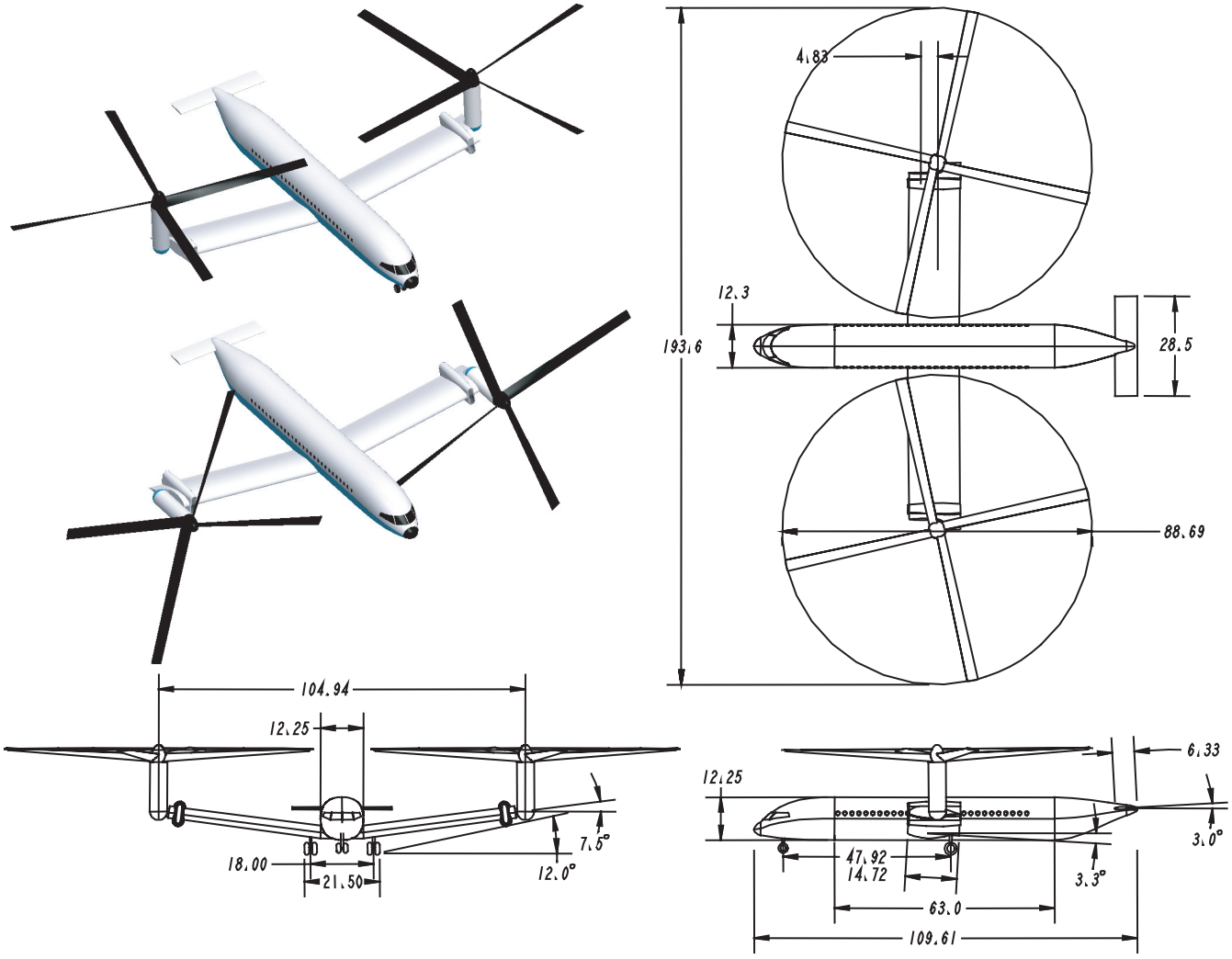

Fig. 1. LCTR concept design (dimensions in ft and deg).

Table 1. Design values for LCTR (Ref. 1).

Design Specification	Value
Cruise speed, knots	350
Cruise altitude, ft	30,000
Hover altitude, ft	5000 (77° F)
Tip speed, hover, ft/sec	650
Tip speed, cruise, ft/sec	350

Baseline Design	Result
Gross weight, lb	123,562
Rotor weight, lb	13,714
Wing weight, lb	8804
Engines and drive train, lb	18,373
Mission fuel, lb	13,624
Rotor radius, ft	44.3
Number of blades	4
Rotor solidity	0.0881
Rotor taper (root/tip chord)	0.8
Precone, deg	6.0
Disk loading, lb/ft^2	10
Length, ft	110
Wing span, ft	105
Wing area, ft^2	1545
Wing loading, lb/ft^2	82
Drag D/q, ft^2	37.3
Engine power, hp	4×6914

Table 2. NASA civil heavy-lift mission (Ref. 1).

Payload	120 passengers = 26,400 lb (with baggage)
Range	1200 nm
Cruise	Mach 0.6 at 30,000 ft (350 knots)
Sustained OEI cruise	at or above 22,000 ft (icing)
Takeoff OEI at Denver	5,000 ft ISA + 20° C
All weather operations	CATIIIC SNI
Community noise	SOA –14 EPNdb

The rotorcraft design software RC performs the sizing of the rotorcraft, including mission performance analysis, and the comprehensive analysis CAMRAD II is used for rotor performance optimization and loads and stability calculations. RC was developed by the Aviation Advanced Design Office of the U. S. Army Aeroflightdynamics Directorate (AFDD), RDECOM (Ref. 5). CAMRAD II is an aeromechanical analysis for rotorcraft that incorporates a combination of advanced technologies, including multibody dynamics, nonlinear finite elements, and rotorcraft aerodynamics (Ref. 6). Other codes, such as NASTRAN and HeliFoil, are used for subsystem analyses. Reference 1 discusses the integration of the various design tools and methodologies into a global design process. For convenience, rotor and wing design are discussed in separate sections of this paper.

Performance requirements are derived from the NASA mission (Table 2) and are used by the RC sizing code to define the basic design. CAMRAD II then optimizes the rotor for performance. Rotor loads determine the rotor structural design. The wing structural design is derived from FAA certification requirements (Ref. 7). FAA requirements also set the aeroelastic stability boundary (whirl-flutter margin), which is checked for compliance by CAMRAD II.

LCTR Sizing

The sizing of the LCTR is described in detail in Ref. 5; key design considerations are summarized here. In contrast to current practice (e.g., V-22), the LCTR has a low-mounted wing (Fig. 1). The advantages over a high wing are a lighter, simpler structure to carry landing gear loads between fuselage and wing; no sponsons needed for landing gear, hence lower drag; and a potential reduction in download, resulting from elimination of the fountain flow over the fuselage (see Ref. 2). Associated design requirements include fixed engines with tilting shafts, longer rotor shafts or large dihedral to place the disk plane above the fuselage in hover, and hingeless rotors for adequate pitch control power in hover. (Cargo/military designs may retain a high wing to meet special requirements, e.g., folding.)

There is no vertical tail, and the rotors provide yaw control. All fuel is carried in the wing. To alleviate tip noise, there is a two-foot clearance between the rotor tip and fuselage in airplane mode (twice the V-22 clearance).

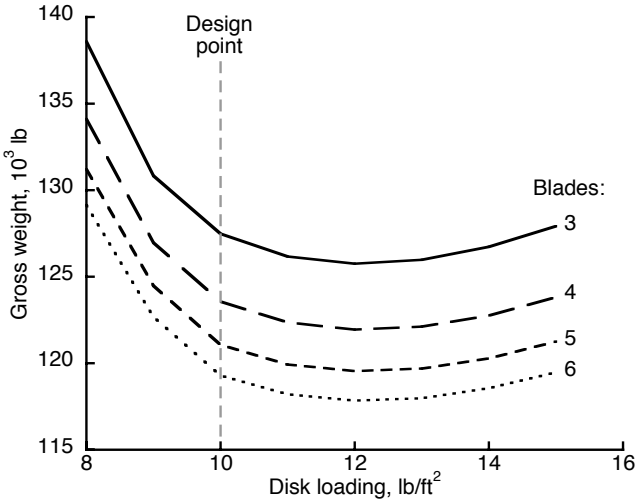

Fig. 2. Sizing sensitivity of gross weight to disk loading and number of blades.

Fig. 2 shows the results of disk loading optimization by RC. Accuracy of the calculations for large numbers of blades is unverified, but the trend is consistent: there is little sensitivity to disk loading above 10 lb/ft^2. The design value of 10 lb/ft^2 was determined by balancing cruise power with

OEI power requirements. This is a lower disk loading than would be expected by merely extrapolating current technology to an LCTR-sized aircraft.

Fig. 2 also shows a decrease in weight with increasing blade number. This is an result of the impact of blade anti-icing requirements on RC's design optimization.

A key technology assumption is that a two-speed transmission will allow a large spread between hover and cruise tip speeds (650 and 350 ft/sec, respectively). Note also the requirement for OEI operation at 5,000 ft (Table 2), which favors low disk loading. Details of the tradeoffs between tip speeds, disk loading, transmission weight and other factors are given in Ref. 5.

LCTR Rotor Design

A major motivation of the present research is to understand the effects of very large size on rotor dynamics, i.e. scaling effects. Simply scaling up an existing rotor design to the size of the LCTR would result in unacceptable weight. However, for a given tip speed, a larger rotor will have a lower rotational speed. This allows blade frequencies to be lower in absolute frequency (Hz) while remaining high in relative frequency (per revolution). This implies that very large rotors could be built at lower weight than current technology allows. It is also consistent with the RC sizing methodology that results in relatively low optimum disk loading (Fig. 2).

A hingeless rotor is the hub concept considered here, because of its simplicity and good stability. It is also compatible with a low-wing design. However, the high loads associated with such a design will require either an unusual blade design or active loads control.

Figure 3 schematically illustrates the design procedure (a similar procedure for the wing design is discussed in the LCTR Wing Design section, below). The process accommodates design requirements in addition to the basic mission specifications. For example, rotor tip speed (Table 1) is set by noise requirements in hover and efficiency requirements in cruise. The RC design code then determines the rotor radius and solidity required to meet the mission requirements in Table 2; the entire aircraft is sized simultaneously with the rotor. Rotor performance capability is derived from scaling rules and technology factors by RC. For example, drag is scaled from historical trends, with an additional factor representing new technology.

The rotor defined by RC is then aerodynamically optimized by CAMRAD II. Twist, taper and precone are determined by selecting the optimum performance values from a large matrix of CAMRAD II analyses that cover both cruise and hover. The blade load-carrying structure is then designed to meet the loads calculated by CAMRAD II. The blade structure is designed using a specially modified version of the NACRA structural design software (Refs. 8, 9).

If needed, the rotor can be reoptimized without resizing the aircraft (inner loop of Fig. 3). To begin another design optimization cycle, RC is recalibrated to match the detailed CAMRAD II predictions for the current design. The aircraft and rotor are then re-sized and the components re-optimized.

There is an option to add new, purpose-designed airfoils after initial optimization. The airfoils are generated by the HeliFoil design code (discussed in the next section). Each airfoil design is driven by the local flow conditions computed earlier in the optimization cycle. This typically requires another cycle of rotor optimization (inner loop) to maximize the benefits of new airfoils.

Because the design process is intended to support research, not production design or certification, its application to the LCTR can be freely modified as the design progresses. Steps may be repeated whenever the results raise particular questions of research interest, or skipped if a previous iteration reaches an optimum or limiting value. The results presented here focus on subsystem optimization (rotor performance and rotor/wing stability) and do not include any complete design iterations beyond those reported in Refs. 1 and 2.

For this report, rotor optimization, aeroelastic stability, and other results were recomputed with CAMRAD II using trim criteria revised in order to better reveal trends in the data. This resulted in occasional, minor changes in the optimized values of FM, η and other parameters, compared to previous results (e.g., Refs. 1-4). The differences were small, so a full reoptimization was not worthwhile. Airfoil tables matched to hover or cruise Re were used throughout.

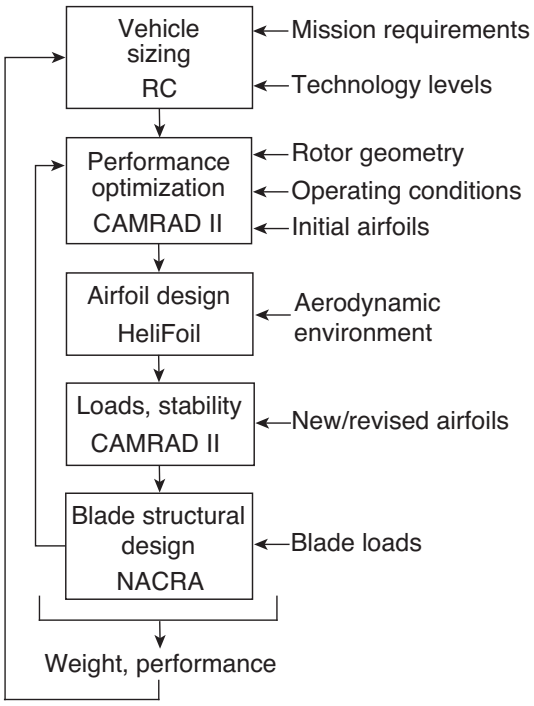

Fig. 3. Iterative rotor design process.

Airfoil design

The airfoil design package HeliFoil was developed by AFDD (Ref. 10). HeliFoil links the following codes to achieve comprehensive airfoil design, optimization and analysis:

MSES v3.0 for transonic airfoil analysis
LINDOP multi-point design optimizer
Eppler PROFIL98 for conformal mapping airfoil design

During the initial pass through the design process, CAMRAD II computes the airfoil operating environment that drives the rotor airfoil design and produces initial estimates of twist and taper. Once the airfoils are designed, CAMRAD II reads in airfoil section characteristics from external tables. For the analyses reported here, two sets of airfoil tables were generated with MSES, one each matched to hover and cruise Reynolds numbers.

Figure 4 shows the LCTR airfoil profiles; Table 3 lists key design values. Each airfoil was designed to operate over a range of radial locations in both hover and cruise. As a result, there are four design points shown for each airfoil, with two radial stations for hover and two for cruise. The airfoils share common design points at 0.45R and 0.75R. In addition, the target pitching moment constraint is shown for each airfoil. The tailored pitching moment distribution uses a strategy of cambered inboard airfoils offset by reflexed outboard airfoils. These points show the airfoil performance compromise between hover and cruise over the specified range of radial stations.

A major challenge for the LCTR rotor airfoil design was to achieve high lift root sections without suffering wave drag in cruise from excessive thickness, or in some cases shock boundary layer separation. The root section used an aft-loaded design with a special leading edge that achieved high lift while preventing supersonic flow in cruise. The outer blade sections were a severe compromise between preventing supersonic flow (and the associated wave drag and shock boundary layer separation) and achieving high lift-to-drag ratio in hover for optimum Figure of Merit at the design weight.

For a production rotor, blending of airfoils along the radius will be required. Because each airfoil is designed to work at the endpoints of its radial extent, the blended airfoils should maintain good performance.

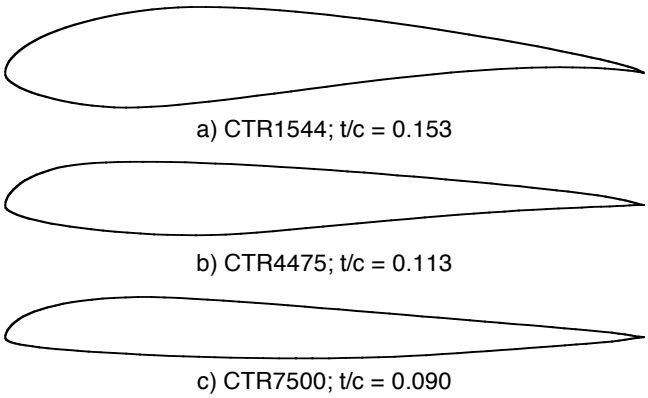

Fig. 4. LCTR airfoils.

Twist optimization

With the newly designed airfoils in hand, the rotor was first optimized for twist. Once past the initial design iteration, twist has minimal further impact on rotor structural requirements. Therefore, twist could be optimized separately from taper and precone. Initial optimization cycles were based on current-technology (SOA) airfoils (Ref. 11), and taper and precone were chosen to reduce blade loads, not to maximize performance (Ref. 2). A taper ratio of 0.8 and 6-deg precone were used for all twist optimizations reported here for the new airfoils and to generate the baseline values in Table 1. The taper ratio is defined as the root chord divided by the tip chord.

Bi-linear twist was used: one linear twist rate was applied from the blade root to 50% radius, and a different linear twist was applied from 50% radius to the tip. A large matrix of combinations of inboard and outboard twist rates was analyzed to map out the design space (Fig. 5). CAMRAD II calculated the resulting performance in hover and cruise. Hover figure of merit (FM) and cruise propulsive efficiency (η) were chosen as metrics to drive the optimization and to illustrate the results. A free-wake model was used for all optimization analyses. The rotor was trimmed to hover $C_T/\sigma = 0.156$ and cruise $C_T/\sigma = 0.073$.

Table 3. Tiltrotor airfoil design conditions.

Airfoil		Position	Hover (5000 ft/77° F)			Cruise (30,000 ft/std)		
Section	c_m	r/R	c_l	M	Re	c_l	M	Re
CTR1544	-0.160	0.15	2.00	0.09	1.86×10^6	0.08	0.60	6.00×10^6
CTR4475	+0.027	0.45	1.28	0.26	4.90×10^6	0.16	0.61	5.80×10^6
CTR7500	+0.014	0.75	0.96	0.42	7.40×10^6	0.21	0.65	5.70×10^6
		0.99	0.41	0.53	8.80×10^6	0.05	0.68	5.70×10^6

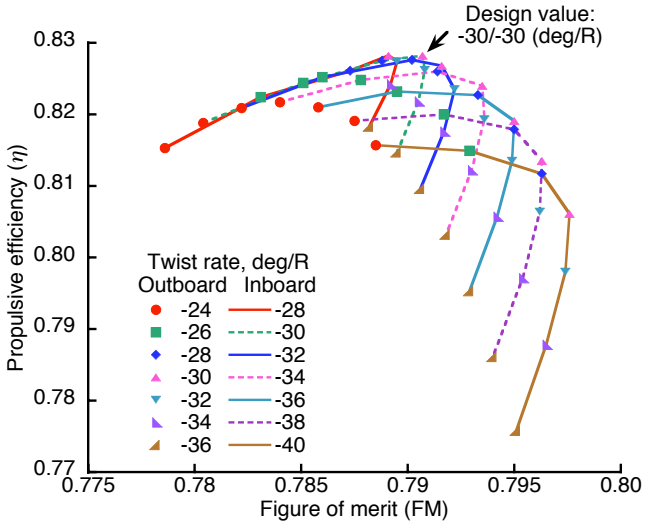

Fig. 5. Twist optimization map for new airfoils, with baseline taper and precone.

The optimum twist lies somewhere along the boundary of the map in Fig. 4, between the peak value of η and the maximum value of FM. The exact location depends upon the weighting of hover versus cruise, as determined by the mission specifications. Ideally, all twist combinations along the boundary, matrixed with all combinations of taper and precone, would be fed back through the full design optimization process (Fig. 3), in order to apply the full mission model in RC and to re-size the aircraft to take full advantage of any performance improvements (or to compensate for shortfalls). However, that would result in every point representing a different aircraft, making direct comparisons impossible.

To narrow the range of values to be further analyzed as the design is refined, a simple efficiency metric was devised. It is the fuel consumed during the nominal mission (Table 2):

$$F_c = \text{power} \times \text{SFC} \times \text{time on condition (hover + cruise)}$$

This formula ignores fuel consumption in climb. A further simplification is to assume constant SFC at each condition, hover and cruise, consistent with a variable-speed transmission (Ref. 2). Because the mission specifications require long range, most of the fuel is consumed in cruise. Despite the simplifications, the formula is fully adequate to discriminate between the effects of different rotor design values. A full-mission, nonlinear optimization will require iteration between RC and CAMRAD II.

The combination of low disk loading in hover and a heavily cruise-weighted mission placed the optimum twist at peak propulsive efficiency (Fig. 5). With the new AFDD airfoils, the optimized values of FM and η improved upon the SOA airfoils, primarily in propulsive efficiency (Table 4) and comfortably exceeded the values achieved during earlier optimizations (FM = 0.780 and η = 0.812; Ref. 1). The relatively slow cruise rpm resulted in a low (for a tiltrotor) twist rate, which is the same inboard and outboard, or 30-deg linear twist root to tip. This is a major change from the XV-15, V-22 and BA-609 rotors.

Table 4. Twist optimization results for 6-deg precone and 0.8 taper (airfoil tables matched to Re).

Optimum Value	LCTR
Inboard twist, deg/radius	-30
Outboard twist, deg/radius	-30
AFDD airfoils:	
Figure of merit	.791
Propulsive efficiency	.828
SOA airfoils:	
Figure of merit	.789
Propulsive efficiency	.820

Figure 6 shows the boundaries of twist maps for AFDD and SOA airfoils. The SOA airfoils were limited to 18% maximum t/c, in order to avoid excessive inboard drag. For purposes of comparison, a special set of airfoil tables was generated for the SOA airfoils for cruise operating conditions, again using MSES. These tables were generated assuming 15% chordwise laminar flow to match the assumptions used for the purpose-designed AFDD airfoils.

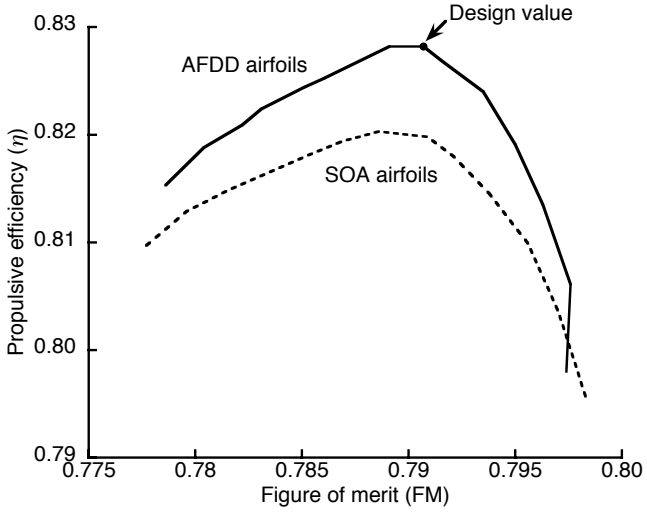

Fig. 6. LCTR twist optimization maxima for two airfoil families.

Compared to the SOA airfoils, the new airfoils yielded a performance improvement of roughly 0.01 η. This should not be interpreted as indicating any deficiencies in the SOA airfoils, because they were designed for different operating conditions (Ref. 11). Nevertheless, newly designed airfoils should provide improvements in performance. Keep in mind that for such large aircraft, even a tiny increase in efficiency can amount to significant improvements in payload or range.

It should be emphasized that neither twist optimization plot (Figs. 5, 6) represents a complete system optimization,

and that further performance improvements may be expected from new airfoil designs, especially if pitching moment constraints are relaxed.

Blade stiffness

The optimization was repeated with rigid blades, yielding a substantial improvement in FM but a very slight reduction in η (Fig. 7). Twist optimizations with flap and torsion stiffness separately increased by an order of magnitude are also shown in Fig. 7. At the scale of this plot, performance with 10× lag stiffness is nearly indistinguishable from the nominal blades and is not shown. These blades represent extreme extrapolations of current structural technology (in contrast to physically impossible rigid blades). It is evident that the hover performance improvement for rigid blades is due almost entirely to flap stiffness. However, the blades had already been stiffened in torsion for stability (Ref. 9), so this conclusion is not universally applicable to other designs.

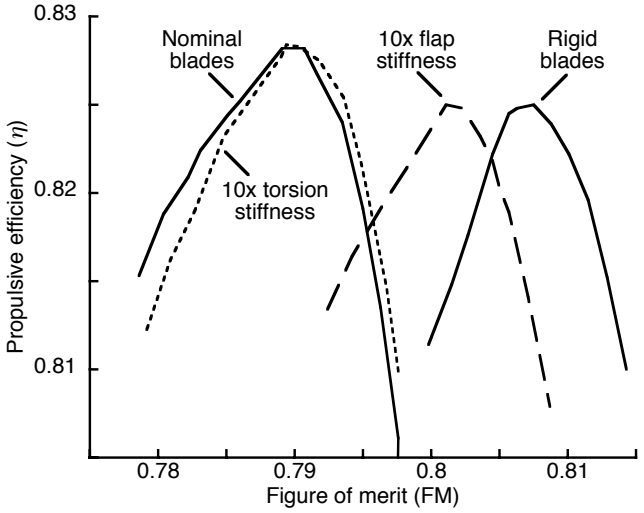

Fig. 7. LCTR performance cost/benefit of blade elasticity.

These results are reasonable, given the source of the performance improvement. With very light blades, there is less centrifugal force than a conventional rotor, hence more coning in hover. The coning angle may be small, but the cumulative losses from inboard tilt of the thrust vector, reduction in effective radius, and wake geometry distortion are important. Blades with increased flap/lag stiffness will have less elastic coning and less resulting lift loss. Without blade flexibility, there is no elastic coning and no lift loss. The exact magnitude of loss will of course depend upon the design value of precone. Stiffer blades would increase blade weight and loads; these penalties would have to be traded against the performance gains and vehicle weight (especially engine power and weight).

A slight increase in cruise performance is provided by flexible blades, compared to stiffer blades (Fig. 7). Because minimum blade stiffness is determined by loads, this effect cannot be safely exploited to improve cruise efficiency. However, because the LCTR is so sensitive to cruise efficiency, it is conceivable that hover efficiency could be sacrificed in exchange for a more benign loads distribution, allowing lighter or more flexible blades, with a resulting increase in cruise efficiency. This effect, should it be realizable, would be dependent upon blade taper and precone, discussed immediately below.

Taper and precone optimization

Taper and precone are structurally related, because both affect rotor loads, which determine blade structural weight, and because taper has an important effect on blade structural efficiency. The connection between rotor loads, structural efficiency and weight means that taper and precone cannot be independently optimized. Here, taper and precone are aerodynamically optimized together; the results determine the performance boundary against which structural tradeoffs must be made as the LCTR design evolves.

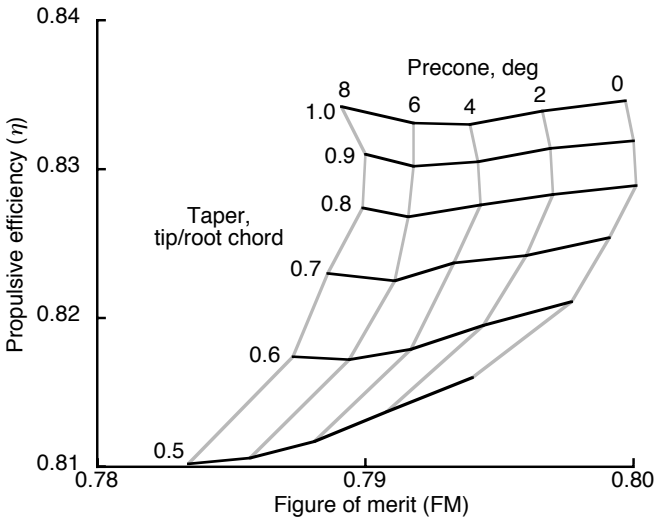

Fig. 8. Taper/precone optimization for the LCTR rotor.

Figure 8 shows the taper/precone aerodynamic optimization for the LCTR, given the optimum twist of -30 deg. As taper was varied, thrust-weighted solidity was held constant at the value in Table 1 (constant chord at 75% radius). The aerodynamic optimum is zero precone with no taper. At maximum performance (the upper right corner of Fig. 8), the aerodynamic effects of precone and taper are nearly independent: η is only weakly affected by precone, and FM shows little effect of taper. There is a subtle peak in FM at a taper of 0.8 and a slight drop in η near 4-deg precone.

Pure aerodynamic optimization would suggest inverse taper. Inverse taper has been proposed for high-speed tiltrotors to reduce root drag (Ref. 12). Figure 8 also implies that negative precone would be beneficial: it would partially

cancel the deleterious effects of elastic coning. However, inverse taper would be extremely challenging to implement, and negative precone presents severe difficulties for aircraft layout (although drooped tips can provide similar benefits). In any case, the design values are limited by blade loads (Ref. 1). The design values of 0.8 taper ratio and 6-deg precone are well short of the aerodynamic ideal.

For the analyses shown in Fig. 8, the stiffness characteristics of all blades were the same, so the optimization map is not definitive: the more highly tapered blades did not benefit from increased stiffness, nor were they penalized for lighter weight (both stiffness and mass reduce elastic coning in hover). Also, airfoil section thickness/chord was fixed for all calculations. Nevertheless, the aerodynamic effects are clear.

Despite the obvious improvements provided by optimizing twist, taper and precone, the net effects on total aircraft performance were limited. The difference in fuel burn between the best and worst twist combinations of Fig. 5 was 6.6%; the difference between the most extreme combinations of taper and precone in Fig. 8 was 3.7%. Although not trivial, these improvements should be considered in light of the fact that mission fuel weight is actually less than total rotor weight or propulsion system weight (Table 1). A considerable reduction in either figure of merit or propulsive efficiency could be tolerated if it resulted in a large decrease in rotor or engine weight. Similar considerations apply to the blade airfoils: thicker sections will cause higher drag and reduced aerodynamic efficiency, especially in cruise, but would also allow for a lighter rotor. Less airfoil camber would reduce drag, at the expense of higher control loads. Moreover, all potential effects on stability must be taken into account, which is the subject of the next section of this paper.

LCTR Wing Design

Because whirl flutter and wing download present technology challenges for tiltrotors, the wing design requires careful attention. A tiltrotor wing must accommodate a transmission cross-shaft. For download reduction, the wing must also have full-span, large-chord flaps with very large deflections. The wing is tip-loaded in hover and low-speed maneuvers, and the concentrated tip masses (engines and transmissions) drive the wing structural dynamics. Large in-plane forces generated by the rotors at high speeds can couple with the wing modes to cause whirl flutter. The wing might also accommodate emerging download-reduction technology (e.g., active flow control). Fixed-wing aircraft design practices are inappropriate to meet these collective requirements.

The large bending and torsional stiffnesses required for tiltrotor aeroelastic stability result in wings with unusually thick cross sections, compared with fixed-wing aircraft. Thinner wings have lower drag, but higher weight to carry the same loads. Purpose-designed airfoils are needed to simultaneously maximize aerodynamic and structural efficiency.

A serendipitous fallout of the low-wing configuration is that the required hingeless rotor tends to be less susceptible to whirl flutter, so the wing need not be as torsionally stiff as would be needed with a gimballed or articulated rotor. However, a wing with a tilting shaft and fixed engines will have different maximum design loads (torsion component) than high-winged designs with tilting engines, because the offset between the rotor thrust vector and wing center of gravity will be different. In addition, a hingeless rotor will require a load-alleviation system. For these reasons, the wing and rotor cannot be designed independently of each other.

Wing design process

The wing design process is summarized in Fig. 9. The airframe geometry and gross weight are determined by the RC sizing code. The rotor design is then optimized for performance with CAMRAD II. The RC wing weight estimate is based upon historical trends and scaling considerations (Ref. 5).

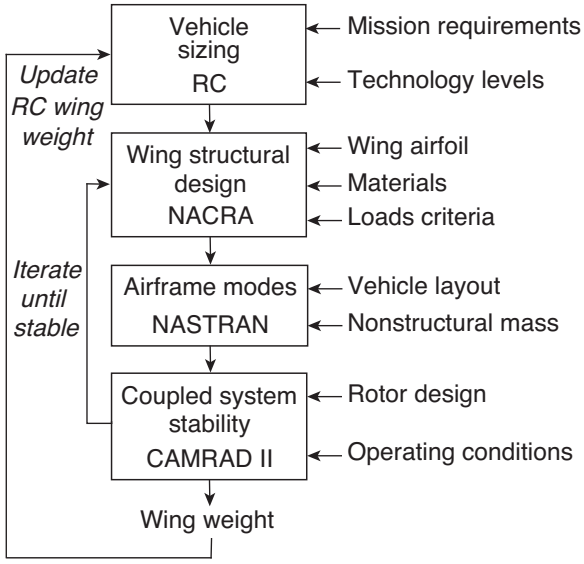

Fig. 9. Iterative tiltrotor wing design process.

The basic LCTR wing structure was generated with NACRA, based on loads requirements. The resulting structural parameters were used to generate the wing elements of a NASTRAN model, which calculated airframe mode shapes and frequencies. CAMRAD II then calculated the coupled rotor/wing stability. If needed for stability, the process was iterated by stiffening the wing. If the weight change imposed by either loads or stability was large enough to significantly change overall airframe weight, the RC sizing code was rerun.

The LCTR wing structural design was driven primarily by 2-g jump takeoff loads and by adequate stiffness to avoid whirl flutter. Table 5 summarizes the design requirements. For this paper, the loads criteria were recalculated from FAR-XX requirements (Ref. 7) instead of being scaled from previous designs, as in Ref. 4, and the wing structure was redesigned for the new loads.

Table 5. Wing structural design requirements.

Purpose-designed wing airfoil (24% t/c), constant chord & section
Spar placement from AFDD designs (Ref. 13)
Loads criteria (RC gross weight):
2-g jump takeoff loads
2-g symmetrical pullout with 75-deg pylons
2.5-g pullout with 0-deg pylons
2.0-g landing/taxi loads
Flutter margin 50% over cruise speed (Ref. 7)
IM7/8552 (graphite)
Tsai-Wu strength criteria, 1.5 factor of safety (Ref. 9)
Non-structural weight allowance for fuel tanks etc. (RC tech factors)

The loads criteria of Table 5 are not definitive. They do not include chordwise loads resulting from yaw inputs in hover; such a loads specification will require development of handling qualities requirements beyond those of Ref. 2. Nor do they include provisions for concentrated landing gear loads, which depend upon the details of the landing gear design. They are intended only for a conceptual-design level of analysis.

The wing structural design process is similar to that for the rotor blades (Ref. 9). The airfoil was designed to give the greatest possible thickness with acceptable drag at the specified cruise conditions (Table 1). The optimum profile for the LCTR wing is shown in Fig. 10. The result is a wing with a very aggressive aerodynamic design. It will require careful attention to gap seals and other design details to be realizable. The payoff is a highly efficient structural design. If anything, the structural requirements of Table 5 are too lenient, and an even more efficient structure than the current design may be appropriate.

A box spar spanning 5% to 55% chord allows for large-chord flaps, a cross-shaft, and other non-load-carrying items. The material used is IM7/8552 (graphite), with the Tsai-Wu strength criteria and a 1.5 factor of safety. Only the load-carrying structure (torque box) was designed here, because it dominated the final wing weight. RC applied additional, non-structural weights based upon the weight of the load-carrying structure. No buckling criteria were applied at the conceptual design level, because that would have required more design details than were available.

The structural properties (composite plies) were tapered from root to tip. The initial tapered design proved aeroelastically unstable, but was stable with doubled beamwise stiffness (perpendicular to the wing chord). The additional stiffness added 830 lb to the wing weight. The combination of more demanding design requirements and a tapered structure resulted in a slight net weight reduction (150 lb) compared to the baseline (Table 1).

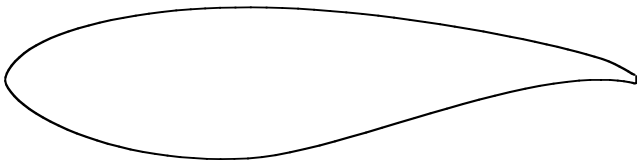

Fig. 10. 24% t/c wing airfoil; note truncated trailing edge.

NASTRAN model

The wing structural properties (inertia, stiffnesses, elastic axis, etc.) were incorporated into a NASTRAN finite element model of the airframe. A simple elastic-line model was used, derived from models developed by AFDD (Ref. 13). It included non-structural wing masses, rigid nacelles with rotor masses, and a flexible fuselage. The model comprised ten elastic wing spar elements and nine elastic fuselage elements. The layout is shown in Fig. 11. The fuselage elements modeled a simplified B-737, to represent worst-case weight and stiffness properties; a state-of-the art composite fuselage would be lighter and stiffer. A rigid, massless tail was included to help visualize the modes. The nacelle model is equivalent to the on-downstop configuration. Based upon this model, the resulting NASTRAN modes were used by CAMRAD II to calculate aeroelastic stability (whirl flutter).

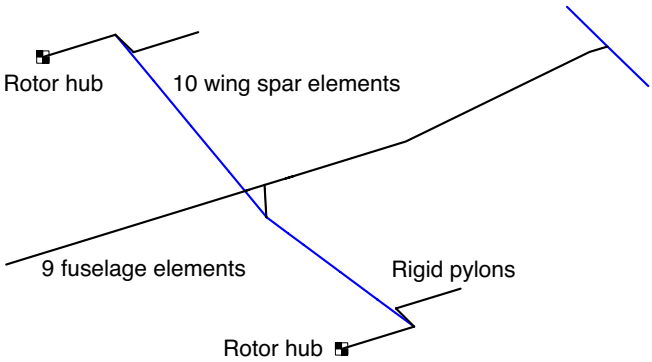

Fig. 11. NASTRAN elastic-line model.

Certain simplifications were applied to the NASTRAN model as appropriate for a conceptual design: there was no wing sweep, and the nacelle center of gravity was assumed to coincide with the wing elastic axis. The nacelle pitch inertia was scaled by RC based on technology factors; for this, there was no differentiation between fixed and tilting engine layouts.

At this stage of the conceptual design process, the airframe structural dynamics model is necessarily very simple, but an elastic-line model is adequate to obtain the low frequency modes that are important for whirl flutter (Ref. 14). The NASTRAN model is also needed for analysis of handling qualities, because low-frequency airframe modes can couple with flight control response.

The resulting modal frequencies are given in Table 6. The first six wing frequencies lie within 1.5 Hz of each other, and four are within 0.5 Hz. This makes conventional wing/rotor frequency placement impossible. Furthermore, all but two of the modes are greater than 1/rev in cruise. Both wing torsion modes are lower in frequency than the bending modes, contrary to the XV-15 and V-22. These are very different design characteristics than apply to any existing tiltrotor, so the wing structure cannot be extrapolated from current (V-22, BA-609) design practice.

Whirl Flutter Analysis

CAMRAD II couples the airframe modes (external inputs) to rotor aeroelastic modes (internal calculations) to get a complete flutter solution. To get a conservative whirl-flutter boundary, the CAMRAD II model assumes structural damping of 3% critical for both the rotor and wing in cruise, but no wing aerodynamic damping (Table 7). The high level of blade structural damping includes a large contribution from the pitch bearing; the value used here is based on experience with hingeless rotors (Ref. 15). The flutter model includes six elastic blade modes, so blade flutter is automatically included in the stability analysis.

For cruise stability calculations, the rotor was trimmed to two conditions known to simulate extremes of whirl flutter behavior: 1) the rotor trimmed to zero power; and 2) the rotor trimmed to thrust equal to aircraft drag up to the speed for maximum power, then trimmed to constant power at higher speeds (equivalent to a powered descent). Stability was calculated for specified mission cruise conditions at 30,000 ft (Table 2).

With this CAMRAD II model for the hingeless rotor and the NASTRAN model for the structurally tapered wing, the LCTR meets the criterion for whirl-mode stability margin of 50% over cruise speed). Because the original design of the current wing required additional stiffening to achieve adequate stability, whirl flutter was the critical design driver for this wing. The wing described in Ref. 4 was less aggressively designed for weight, with the result that its design was driven by loads. The addition of more stringent loads requirements, such as landing gear loads, could shift the structurally tapered wing to a loads-driven design, as could changes in geometry, such as repositioned engine center of gravity.

Table 7. CAMRAD II flutter model.

Cruise Stability
6 elastic modes per blade (trim and flutter)
12 wing/fuselage modes (Table 6)
rigid drive train (rotational inertia, but no shaft flexibility)
3% critical blade structural damping
3% critical wing structural damping
no wing aerodynamic damping
dynamic inflow
symmetric/antisymmetric analysis, 65 modes total

Figure 12 shows example root-locus plots of coupled wing/rotor aeroelastic stability, with symmetric and antisymmetric modes plotted separately. Only the least stable modes are shown. The stability requirement is 150% of design cruise speed, or 525 knots (Table 5). All modes are stable until 530 knots, which is nearly ideal: there is very little excess stability margin, hence minimal excess wing weight. The critical mode is the antisymmetric wing torsion mode. Stiffening the wing moved the coupled modal frequency from just below to just above 1/rev near the stability boundary (Fig. 12(b)). The symmetric beam and torsion modes, near 1/rev and 2/rev, respectively, also have little stability margin (Fig. 12(a)).

Table 6. NASTRAN modal frequencies for LCTR.

Symmetric Modes			Antisymmetric Modes		
Frequency		Mode	Frequency		Mode
Hz	Per rev		Hz	Per rev	
1.73	1.37	Wing torsion	1.85	1.47	Wing torsion
2.62	2.08	Wing beamwise bending	3.07	2.44	Wing beamwise bending
2.75	2.18	Wing chordwise bending	3.21	2.55	Wing chordwise bending
5.45	4.33	Vertical fuselage bending	4.95	3.93	Lateral fuselage bending
8.33	6.61	2nd wing chord	7.82	6.21	2nd wing chord
—	—		9.79	7.75	Lateral tail bending
—	—		11.09	8.80	2nd lateral tail
Cruise 1/rev = 1.26 Hz (75.5 rpm)					

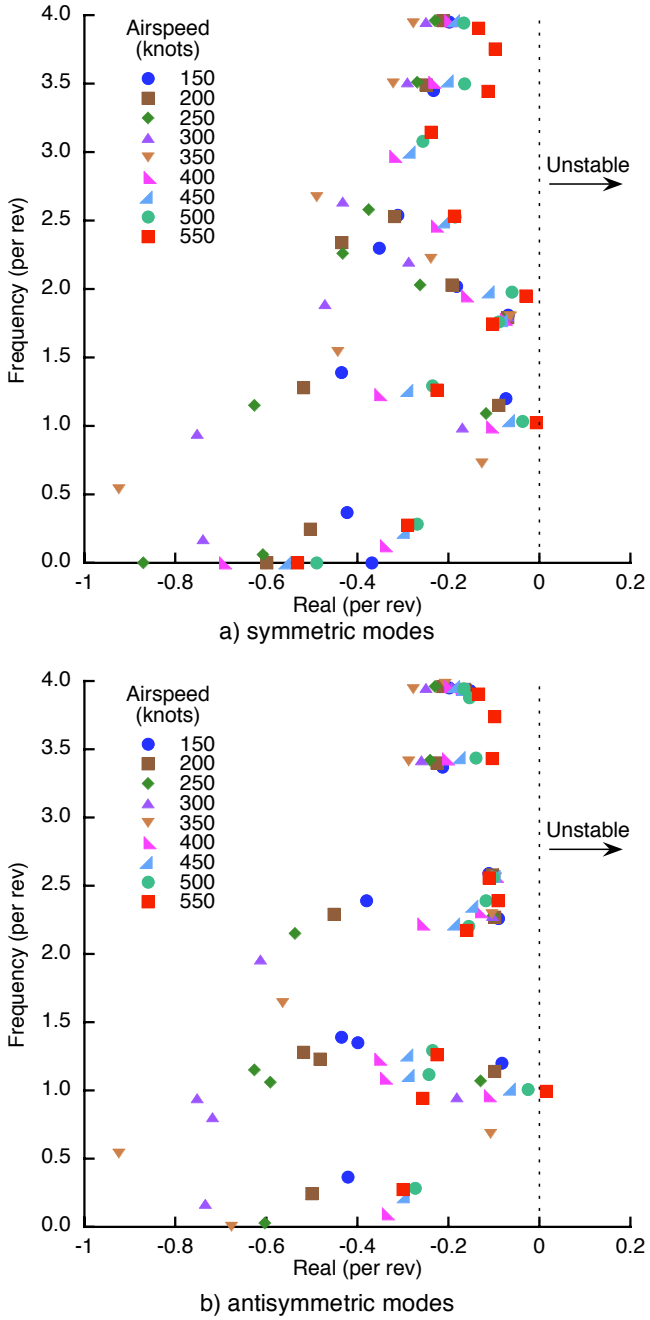

Fig. 12. Example aeroelastic stability (whirl flutter) predictions at 30,000 ft; trim to thrust until 350 knots, then trim to 350-kt power.

Beamwise stiffening was more effective than torsion stiffening for stabilizing the wing torsion modes. Whirl-mode stability depends not only upon frequency, but upon mode shape, and the beam and torsion modes tend to be highly coupled. It is therefore not surprising that off-axis stiffening can be more effective than on-axis stiffening. Moreover, the beamwise modes have near-perfect motion cancellation in the rotor plane at the rotor hubs. This is a purely serendipitous effect and cannot be expected to be realized for other wing/nacelle geometries or for other combinations of rotor and nacelle mass and c.g.

Figure 12 shows the worst-case (maximum power) cruise condition for flutter. The zero-power cases (not shown) are slightly more stable than the maximum-power conditions. This is in contrast to past experience, probably because the low cruise rpm combined with low blade weight greatly reduces the adverse affects of precone, which is usually destabilizing at zero power (negative thrust).

Sensitivity of whirl flutter to taper and precone were checked at 525 knots. Precone and taper were independently varied over the same ranges as in Fig. 8, with no adverse effects on stability. Indeed, for the least stable modes, the differences are not discernable on the scale of Fig. 12. Precone and taper can, therefore, be optimized without any stability constraints.

The stability analyses were repeated with SOA airfoils. The results were generally similar, but with a slight reduction in stability margin. The stability trends (not shown) were erratic at very high speed, which is typical of rotor airfoils with poor transonic behavior. Given that the SOA airfoils were not designed for these operating conditions, a minor reduction in stability is not surprising. An appropriately cautious conclusion is that the AFDD airfoils improved rotor performance with no adverse effects on stability.

Research Recommendations

Several opportunities for research have been mentioned in this report and are collected and expanded upon here. The purpose of these suggestions is not so much to design a better LCTR, as to create a more rigorous baseline against which to evaluate technology developments and to determine the most promising areas of research.

Weight and cost sensitivity factors could be derived from RC for use during component optimization. For example, twist optimization could then be determined by total operating cost, not just fuel burn. Proper optimization would require not just an examination of rotor or wing design, but reliable estimates of manufacturing, maintenance and fuel costs, all extending throughout the lifetime of the aircraft (see Ref. 16 for a discussion of cost methodology). The objective is to more quickly converge on optimized rotor and wing designs without having to resize the aircraft for every parameter variation. This would also make research findings less dependent upon the particulars of the LCTR design specifications.

The obvious next step in rotor optimization would be to explicitly trade off structural weight against aerodynamic efficiency. Higher efficiency might lead to lower total weight even with heavier rotors, so there are further potential tradeoffs between rotor, airframe, and drive train weight, with a parallel effort for the wing.

Ideally, an entire family of airfoils would be developed, with systematic variations in thickness and camber, and with matching blade structural designs. Relaxing the pitching moment constraints would further improve performance. Structural designs for a matrix of values of taper and precone would also be developed. Rotor weight could then be traded off against performance with higher levels of accuracy and realism than was possible here. Such an undertaking would require a more efficient and robust method of generating airfoil tables than is now available, along with a reliable way of scaling blade structural weight with geometry and loads. With unconstrained section pitching moments, control system weight and stiffness will have to be included in rotor optimization and stability analyses. New rotor airfoils carry the risk of different transonic behavior and attendant changes in stability, and different mass or stiffness distributions will affect mode shapes and stability. Both isolated-rotor and whirl-mode stability must be re-examined for any change in rotor airfoils or structure.

The wing loads criteria are expected to continuously evolve, as more design details become available against which to apply more rigorous requirements. An obvious example is to add concentrated landing gear loads. Although a stronger wing will be stiffer, changes in mass distribution and c.g. may change the mode shapes, so it should not be assumed that additional strength will improve whirl-mode stability. Therefore, more sophisticated structural design methods should be considered, including aeroelastically tailored structures. The wing airfoil design should be re-evaluated to explicitly include flaps, flaperons and spoilers, with provisions for track fairings, gap seals, and other details detrimental to performance (in contrast to the current aerodynamic model, which relies on RC technology factors).

It will eventually become appropriate to run the updated rotor and wing performance and weights through the entire optimization process to resize the aircraft. The LCTR could then be redesigned for a higher blade passage frequency (as in Ref. 1), this time with a fully optimized rotor and resized wing. This entails an additional design specification (minimum hover frequency), which will require re-examination of disk loading, solidity and blade number, all of which can be expected to affect the rotor optimization. A redesign may also result in different whirl-flutter margins, which constitute an important design constraint.

Taken all together, the above suggestions would add up to a new vehicle design capability, closely parallel to RC, but less dependent upon extrapolations of historical trends. Advanced engine models, airframe aerodynamics, transmission concepts, and other technological developments are obvious candidates for inclusion.

Conclusions

For very large tiltrotors, rotor and wing design are interrelated. As part of the Heavy Lift Rotorcraft Systems Investigation, a design method was developed that produced a low-drag, structurally efficient wing compatible with a lightweight, aerodynamically efficient, stable rotor. A very large (124,000-lb) civil tiltrotor was designed to carry 120 passengers 1200 nm at 350 knots. The Large Civil Tiltrotor (LCTR) employs a low-mounted wing and hingeless rotors, with very low cruise tip speed (V_{tip} = 350 ft/sec, 75.5 rpm).

New airfoils were designed for the LCTR and their effects on rotor optimization were studied in some detail, with attention focused on twist, taper and precone optimization. Compared to current technology airfoils, modern airfoils can provide improvement in high-altitude, high-speed cruise. Slowing the rotor in cruise resulted in a lower value of optimized twist than existing tiltrotors. Reducing precone and taper resulted in significant improvements in hover and cruise efficiency, respectively, but a realistic design will be constrained by loads and weight. Optimization of the rotor with the new airfoils and structurally-constrained taper and precone resulted in figure of merit of 0.79 and propulsive efficiency of 0.83 at design operating conditions.

Rotor flexibility was highly detrimental to hover efficiency, but slightly beneficial in cruise. Rotor optimization should be extended to include tradeoffs between aerodynamic performance and rotor weight, including the effects of precone, blade stiffness, and taper. A similar extension to airfoil design would relax pitching moment constraints in return for better performance, and would require trading off aerodynamic efficiency against blade weight and control loads. Such research effort would require higher-order optimization methods than used here.

The hingeless-rotor, low-wing concept is feasible, but a wing designed exclusively for loads proved unstable: additional stiffening was required to achieve an adequate whirl-flutter margin. Full power was less stable than zero power, in contrast to conventional designs. Traditional frequency-placement criteria were not appropriate for the wing design, and may be impossible: the first six wing frequencies were within 1.5 Hz of each other (1.73-3.21 Hz), with the lowest wing/nacelle frequency above 1/rev and all but two modes above 2/rev. Rotor precone and blade taper had little effect on whirl-mode stability.

Acknowledgments

The author wishes to thank Wayne Johnson (NASA Ames Research Center) for his initiative and leadership in developing and sustaining the Heavy Lift Rotorcraft Systems Investigation, and for his invaluable guidance in performing design, optimization and analysis of large tiltrotors. Thanks are due to Preston Martin (AFDD), who designed the airfoils and provided descriptive material; Jianhua Zhang (Pennsylvania State University), who generated the rotor and

wing structural designs; and to Gerardo Nuñez (AFDD), who provided the LCTR layout drawings. The author also acknowledges the long history of productive cooperation between NASA and AFDD in all manner of rotorcraft research.

References

1. Johnson, W., Yamauchi, G. K., and Watts, M. E., "Designs and Technology Requirements for Civil Heavy Lift Rotorcraft," AHS Vertical Lift Aircraft Design Conference, San Francisco, California, January 2006.

2. Johnson, W., Yamauchi, G. K., and Watts, M. E., "NASA Heavy Lift Rotorcraft Systems Investigation," NASA TP-2005-213467, September 2005.

3. Acree, C. W., Martin, P. B., and Romander, E. A., "Impact of Airfoils on Aerodynamic Optimization of Heavy Lift Rotorcraft," AHS Vertical Lift Aircraft Design Conference, San Francisco, California, January 2006.

4. Acree, C. W., and Johnson, W., "Performance, Loads and Stability of Heavy Lift Tiltrotors," AHS Vertical Lift Aircraft Design Conference, San Francisco, California, January 2006.

5. van Aken, J. M. and Sinsay, J. D., "Preliminary Sizing of 120-Passenger Advanced Civil Rotorcraft Concepts," AHS Vertical Lift Aircraft Design Conference, San Francisco, California, January 2006.

6. Johnson, W., "CAMRAD II Comprehensive Analytical Model of Rotorcraft Aerodynamics and Dynamics," Johnson Aeronautics, Palo Alto, California, 2005.

7. "Interim Airworthiness Criteria, Powered-Lift Transport Category Aircraft," FAA Draft FAR-XX, July 1988.

8. Floros, M. W., and Smith, E. C., "NREL Advanced Composite Rotor Analysis (NACRA)," Pennsylvania State University, October 2002.

9. Zhang, J., and Smith, E., "Design Methodology and Cost Analysis of Composite Blades for a Low Weight Rotor," AHS Vertical Lift Aircraft Design Conference, San Francisco, California, January 2006.

10. Martin, P. B., "Rotor Blade Airfoil Design for High-Altitude, Long-Endurance VTOL UAVs," 31st European Rotorcraft Forum, Florence, Italy, September 2005.

11. Narramore, J. C., "Airfoil Design, Test, and Evaluation for the V-22 Tilt Rotor Vehicle," 43rd Annual Forum of the American Helicopter Society, St. Louis, Missouri, May 1987.

12. Liu, J., and McVeigh, M. A., "Design of Swept Blade Rotors for High-Speed Tiltrotor Application," AIAA 91-3147, AIAA, AHS, and ASEE, Aircraft Design Systems and Operations Meeting, Baltimore, Maryland, September 1991.

13. Peyran, R., and Rand, O., "The Effect of Design Requirements on Conceptual Tiltrotor Wing Weight," AHS 55th Annual Forum, Montréal, Quebec, Canada, May 1999.

14. Acree, C. W., Peyran, R. J., and Johnson, W., "Rotor Design Options for Improving XV-15 Whirl-Flutter Stability Margins," NASA /TP-2004-212262 and AFDD/TR-04-001, March 2004.

15. Kloppel, V., Kampa, K., and Isselhorst, B., "Aero-mechanical Aspects in the Design of Hingeless/Bearingless Rotor Systems," Ninth European Rotorcraft Forum, Stresa, Italy, September 1983.

16. Coy, J. J., "Cost Analysis for Large Civil Transport Rotorcraft," AHS Vertical Lift Aircraft Design Conference, San Francisco, California, January 2006.